



Research article

**BIOSENSOR PROPERTIES OF PLASMONIC SILVER NANOPARTICLES  
PRODUCED BY THE PLD MECHANISM**

**Ilhan CANDAN<sup>1,2\*</sup>**  **Serap YİĞİT GEZGİN<sup>3</sup>**  **Yasemin GÜNDOĞDU<sup>4</sup>**   
**Hadice BUDAK GUMGUM<sup>1,2</sup>** 

<sup>1</sup> Dicle University, Faculty of Science, Department of Physics, 21280, Diyarbakir, Turkey

<sup>2</sup> Dicle University, Institute of Science and Technology, Department of Physics, 21280, Diyarbakir, Turkey

<sup>3</sup> Department of Physics, Faculty of Science, University of Selçuk, 42031 Selçuklu, Konya, Turkey

<sup>4</sup> Department of Electric and Energy, Kadınhanı Faik İçil Vocational High School, University of Selçuk, 42031 Selçuklu, Konya, Turkey

\*Corresponding author: [ilhan.candan@dicle.edu.tr](mailto:ilhan.candan@dicle.edu.tr)

**Abstract:** Plasmonic metal nanoparticles (NPs), such as Ag, Au, Cu NPs, attract great interest due to their notable applications in biological, and chemical sensing. Researchers have studied the plasmonic metal NPs which have exceptional optical properties in a large spectral region. Metal NPs form a unique surface plasmon resonance (SPR) peak that is in the electromagnetic spectrum's visible part. The peak of SPR firmly depends on the NP's size, shape, dielectric constant, and medium that the particle is in. Light interacts with nanoparticles that are smaller than the wavelength of incident light in localized surface resonance. That leads Localised Surface Plasmon Resonance (LSPR) in which an oscillating local plasma around the NP with a certain frequency form. The LSPR detection is the most common method for wavelength shift measurement. Since analyte absorption causes a significant change on the value of local dielectric constant, the LSPR peak shifts. It is known that biological molecules such as proteins and antibodies can sensitively be detected while they affect the local dielectric environment. Therefore, Ag or Au based metal NPs can be used as a sensor with the help of LSPR wavelength shift technique. Among the metal NPs, Ag has a relatively higher refractive index sensitivity. Moreover, Ag NPs generate measurements that are more precise since they have a sharper LSPR peak. In our work, we produce plasmonic Ag NPs with various sizes and spherical shapes by making use of the Pulsed Laser Deposition (PLD) mechanism. Subsequently, we have investigate the LSPR peaks of these NPs via the UV-Vis spectroscopy. Additionally, biosensor properties of plasmonic Ag NPs are investigated by binding Protein A molecules to surface of the NPs. It is significant to mention here that we obtain an LSPR wavelength shift, which has a value around 100 nm/RIU.

**Keywords:** Plasmonic nanoparticles; Silver nanoparticles; LSPR; PLD, Plasmonic sensor

Received: October 21, 2021

Accepted: December 22, 2021

## 1. Introduction

Nanoparticles (NPs), which attract attention with their small-scale dimensions, strong absorption coefficients, large surface area/volume ratios, find a lot of importance in analytical chemistry [1, 2]. Analytical techniques built on NPs not only take vital roles in the detection widespread significance in in the fields of pharmaceutical, clinical, food safety, and environmental because of their simple structures, wide linear ranges, and high sensitivity. Therefore, metal nanostructures are of great interest, both fundamentally and technologically, due to their unique functionality and properties in contrast to their large counterparts. In addition to this, optical features of the NPs have important aspects. Many

metal structures such as nanoscale gold and silver perform great absorption in the visible spectrum compared to their bulk structures. The standard absorption peaks of Au and Ag elements are around 520 and 400 nm, respectively. The nanoscale metal particles' optical properties varies by numerous parameters such as their size [3], shapes [4], metal composition [5], and environment of the nanoparticles [6-10]. In many research areas, the metal NPs play significant roles. For instance, the effects of quantum restrictions on electronic, magnetic, and other related features can be investigated by making use of an experimental model of the NPs [11, 12]. Additionally, the metal NPs are additionally employed in various fields such as catalysis [13], photography [14], biological labelling [15], photonics [16], optoelectronics [17], information storage [18], as well as the surface enhanced Raman scattering (SERS) [19, 20]. It is generally known that the metal NPs may be produced via several methods such as electrochemical techniques, organometallic precursors' decomposition, and metal salts' reduction or vapour deposition in the presence of stabilizers, especially the Laser Ablation (LA) and the Pulsed Laser Deposition (PLD). In these techniques, the nanoparticle size and density can be adjusted to the desired scale by easily controlling the parameters (for example laser fluency, wavelength, pulse number, pulse duration, pressure of background gas and distance from substrate to target, substrate temperature) of PLD system. Thanks to these distinctive features of PLD, the movement of LSPR peaks of plasmonic nanoparticles in the short or long wavelength direction of the solar spectrum can be easily achieved.

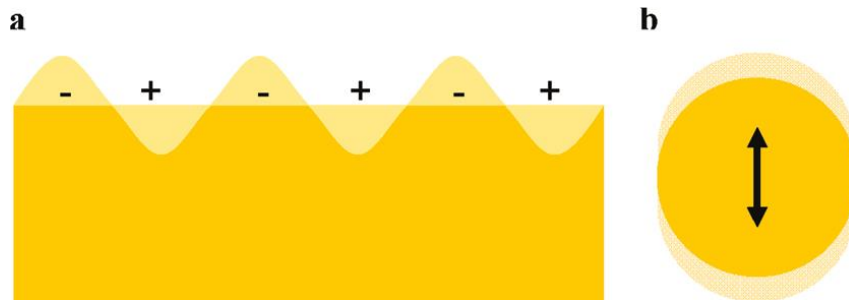


**Figure 1.** Illustrations of a) surface plasmons and b) a localized surface plasmon[21].

The plasmonic metal NPs' optical properties are very important because of the SPR phenomenon. The SPR corresponds to oscillation frequency of the conduction electrons in results of the electromagnetic radiation's electric field. As shown in Figure 1, surface plasmons are produced by oscillations of free electrons within the metal as result of electromagnetic waves that are trapped in the interface between metal and dielectric parts. The Mie theory explains this phenomenon successfully via the Maxwell equation [22]. The SPR peak is generated by considering material's negative real and positive imaginary dielectric constants. On the other hand, the SPR is a harmonic oscillation of electrons in the surface of metal NP and stimulated by electromagnetic field in the optical region. Consequently, the resulting signal is considerably strengthened.

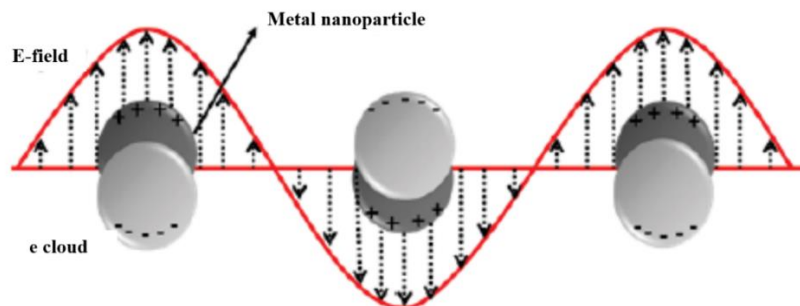


**Figure 2.** Schematic representation of plasmon oscillations demonstrating the relative displacement between the cloud of electron and nuclei.

Light interacts with smaller nanoparticles compared to the wavelength of incident light in the localized surface plasmon. As shown in Figure 2, the results in the formation of a local plasma around the nanoparticle, which has a frequency named as the localized surface plasmon resonance (LSPR). As a matter of fact, the LSPR is similar to the SPR and has a high sensitivity when changes occur in the local dielectric environment [23]. The LSPR wavelength shifts are generally detected through changes occurring in the local environment, and an angularly resolved sensing is possible for the LSPR mechanism [24].

The way how metal NPs interact with electromagnetic radiation is explained quite well by Mie's scattering theory utilizing Maxwell's equations. It mainly expresses the optical extinction for the metal NPs that has a smaller radius compared to the incident radiation's wavelength ( $2r \ll \lambda$ ) [25]

The biosensors, development is very significant for the analysis and detection of numerous chemicals, toxic substances, as well as biologically crucial compounds, which are used in the environmental monitoring, clinical, food safety and safety. Recently, for the development of biosensors, the SPR has been utilized [26, 27]. The interaction of unlabelled biomolecules can be detected by the SPR biosensors; thus, they can be used to detect unlabelled biomolecules. For this reason, the SPR biosensors are widely used in interaction studies and in receptors, carbohydrates, proteins, cells, different forms of bacteria, clinical diagnosis, military defence. Due to its good detection sensitivity, outstanding features such as unlabelled and detection in the real-time, the SPR biosensors are employed in various applications, for instance, bacteria, pesticides, allergens, and viruses' detection. Varying on the target sample's size, four distinct test formats have been developed for the SPR-based biosensors, which are used in the direct testing, competitive testing, sandwich testing and inhibition testing mechanisms [28-31].

In this paper, plasmonic Ag nanoparticles were produced by using the PLD method. The produced plasmonic Ag nanoparticles' LSPR peak are measured by the UV-Vis spectrometer. The LSPR peaks of 12600 and 14400 laser pulse Ag NPs were found to be at 680 and 700 nm, respectively. The morphological of the Ag NP thin films were investigated by Scanning Electron Microscopy (SEM) method and composition of the thin films were analysed by the Energy Dispersive Spectroscopy (EDX) technique. Shape of the produced Ag NPs were measured to be sphere and the size of that was found to be ranging from one to few hundreds nm. Additionally, biosensor properties of Ag NPs were investigated by binding protein A to NPs' surface.

## **2. Materials and Methods**

### **2.1. Experimental Setup**

The PLD system was used to produce silver nanoparticles. Nd:YAG laser (Continuum, Minilite II) system was operated and had pulsed mode with duration of 5 ns and repetition rate of 10 Hz at 1064 nm. The laser system has a capability of producing second, third, and fourth harmonics for 1064 nm, which are 532, 355, and 266 nm, respectively. In this work, 1064 nm fundamental wavelength had been employed. A neutral density filter was used to control laser pulse power that was measured before focusing lens as shown in Figure 3a. A glass microscope slide was used as a substrate to deposit Ag NP on. To clean the glass microscope slide, firstly, soap foam was applied, and then, it was bathed in isopropyl alcohol and acetone for 15 minutes each step. After that, the substrates were placed in an ultrasonic bath to further the cleaning process. Lastly, a nitrogen gas flow was used to dry the substrates. In our experiment, we utilized commercially available silver sputtering target with high purity (99.99%, Plasmaterials, USA). In order to avoid any damaging effect, the target and substrate were located on two independently rotating holders. As each laser pulse hit different part in the target, a homogeneous coating was achieved after laser ablation process as illustrated in Figure 3b.

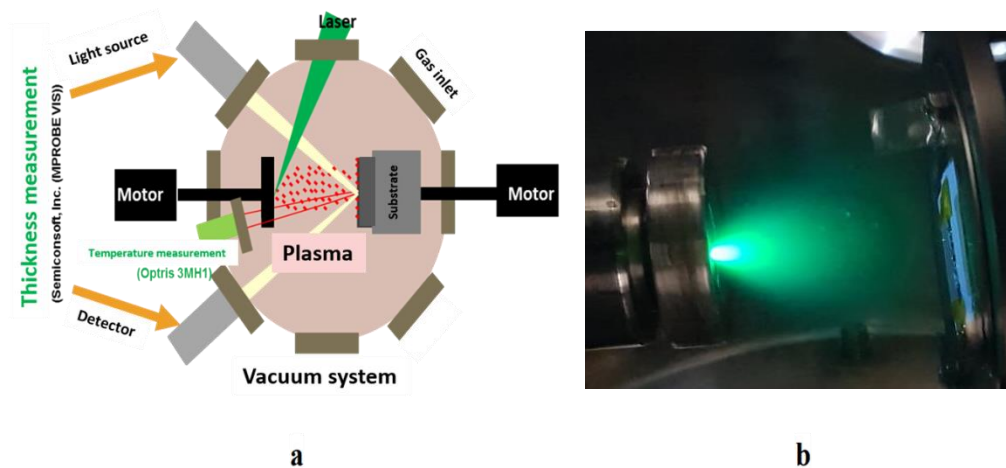


**Figure 3.** a) Schematic view of the PLD system designed and manufactured locally by the Laser spectroscopy group of Selcuk University, b) Plasma of the ablated Ag target material, using the PLD system.

5 cm fixed distance was applied between the target and substrate parts. Subsequently, Laser deposition process was carried out at room temperature for all films. The energy of laser was set to 35 mJ per pulse and the laser beam was focused on Ag target using a lens having 50 cm focal length. The laser beam's angle was fixed to be  $45^{\circ}$  on the target surface. The experiments were carried out in ultra-high vacuum which was around  $5 \times 10^{-7}$  mbar. The silver sputtering target was ablated by applying 12600 and 14400 laser pulses for different nanoparticle production. The produced Ag nanoparticle morphologies was analysed by the SEM measurement and the EDX spectrum was taken to investigate the element composition of the thin film. The Ag nanoparticles' absorption spectra were determined by utilizing a UV-Vis spectrometer (V-670 Jasco, USA). For investigating sensor properties of the produced plasmonic nanoparticles, the protein A (Sigma-Aldrich) solution of 1 ppm was used. Ultra-pure water was used as a solvent. Plasmonic Ag nanoparticles' LSPR peak shifts were measured by the UV-Vis spectrometer.

### 3. Results and Discussion

Plasmonic Ag NP thin films were produced by the PLD. The produced Ag NPs were investigated by the UV-Vis spectrum and the result is shown in Figure 4. As seen from the figure, two LSPR peaks of Ag NPs appear for 12600 and 14400 laser pulses, which are positioned at 680 and 700 nm, respectively. The LSPR peaks of Ag NPs are 680 and 700 nm for 21 and 24 minutes. Both peaks are in the visible part of the electromagnetic spectrum. With the increase in the number of laser pulses, the LSPR peak shifted slightly to the longer wavelength region and their absorption intensity increased.

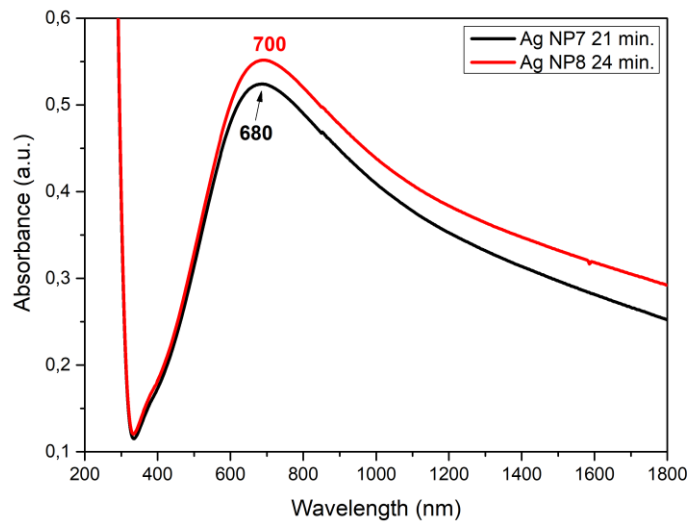


**Figure 4.** UV-Vis spectrum of plasmonic Ag NP produced by PLD for deposition times of 21 (12600 laser pulses) and 24 minutes (14400 laser pulses).

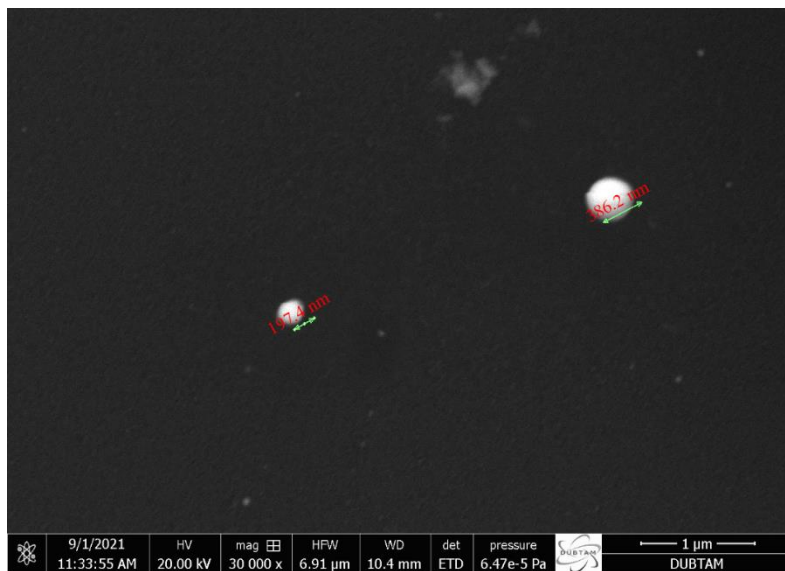


**Figure 5.** SEM image of Ag NP produced by PLD for 21 minutes (12600 laser pulses).

The SEM images of Ag NPs produced by the PLD for 12600 laser pulses are shown in Figure 5. Shapes of the produced NPs are spherical and sizes of them are 197.4 and 386.2 as seen in Figure 5. It should be noted that the imaged NPs are merely chosen for the purpose of illustration. There may be Ag NPs of different sizes in the other parts of the thin film as they are out of focus in the SEM image.

On the other hand, Figure 6 illustrates the SEM image of Ag NPs produced by the PLD for 14400 laser pulses. The shape of these NPs is spherical as well. The size of the NP illustrated in the figure is around 398 nm. Inset picture is the same Ag NP with size of 398 nm. It can be concluded that the NPs produced for 14400 laser pulses are larger than those of produced for 12600 laser pulses. Because, with the increase in the number of laser pulses, the rate of deposition is increased. The increase in the number of Ag nanoparticles deposited on top of each other and side-by-side at high laser pulse, number caused the particle size to increase.



**Figure 6.** SEM image of Ag NP produced by PLD for 24 minutes (14400 laser pulses).

The size of the plasmonic nanoparticles can be calculated by the following equation:

$$d = \frac{\ln\left(\frac{\lambda_{spr} - \lambda_o}{L_1}\right)}{L_2} \quad (1)$$

where,  $\lambda_o = 400$  nm;  $L_1 = 6.53$  nm;  $L_2 = 0.0216$  nm<sup>-1</sup> [32]. Using Eq (1), the nanoparticle size was theoretically calculated to be 174 nm for LSPR peak of 680 nm, while it was obtained 177 nm to the LSPR peak in 700 nm. As in the morphological structure, while the number of laser pulses increased, the particle size expanded with the increase of the long wavelength of the LSPR peak.

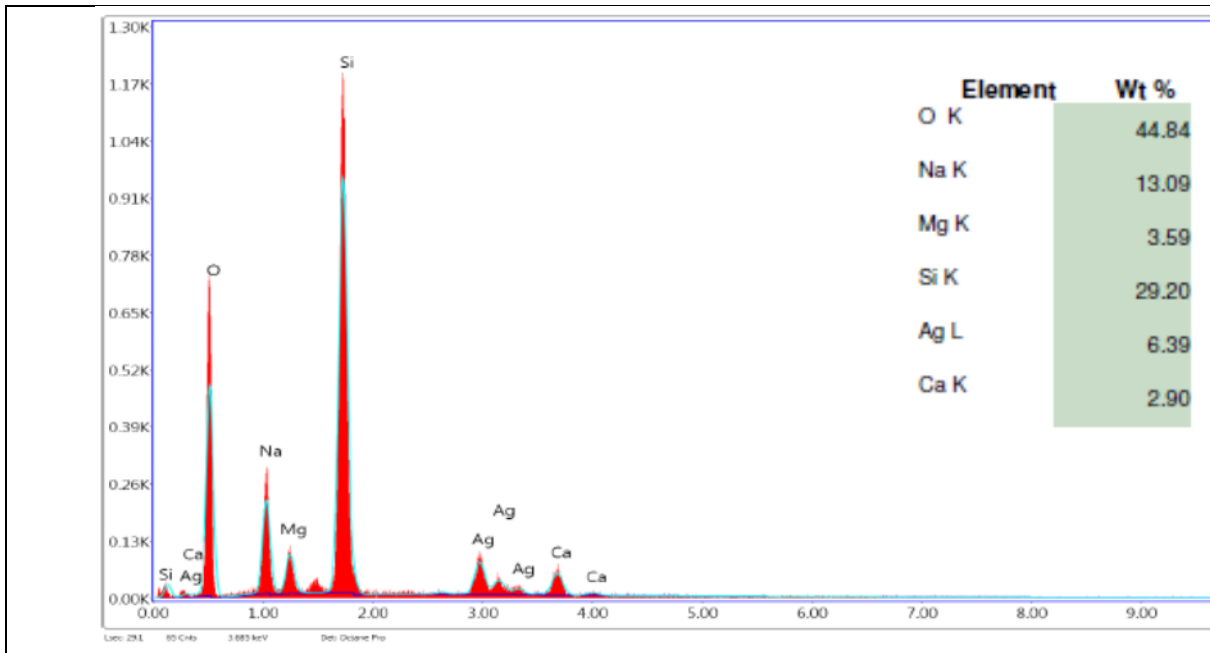


**Figure 7.** EDX spectrum of the Ag NPs produced for 12600 laser pulses.

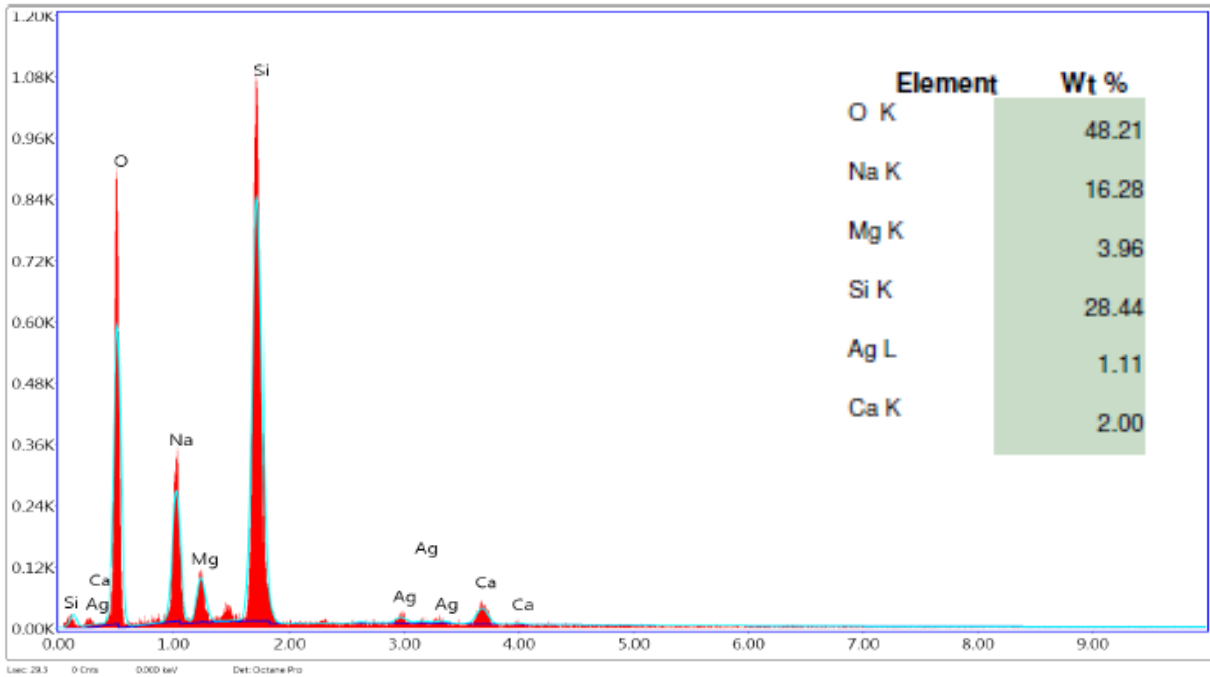


**Figure 8.** EDX spectrum of Ag NP for 24 minutes (14400 laser pulses).

The contents of the elements in the thin films are including Ag, Si, O, Na, Ca, Na, and Mg. Ag content proves that we have used the Ag target for the experiment as well as the other contents as we deposited the NPs on the glass microscopic slides. The wt % of the elements are given in the inset of Figure 7.

The EDX spectrum of Ag NPs produced for 14400 laser pulses are demonstrated in Figure 8. The contents of the thin film are composed of Ag, Si, O, Na, Ca, Na, and Mg. The Ag NPs are deposited in the glass microscope slides and the EDX findings agree with the experimental set up.

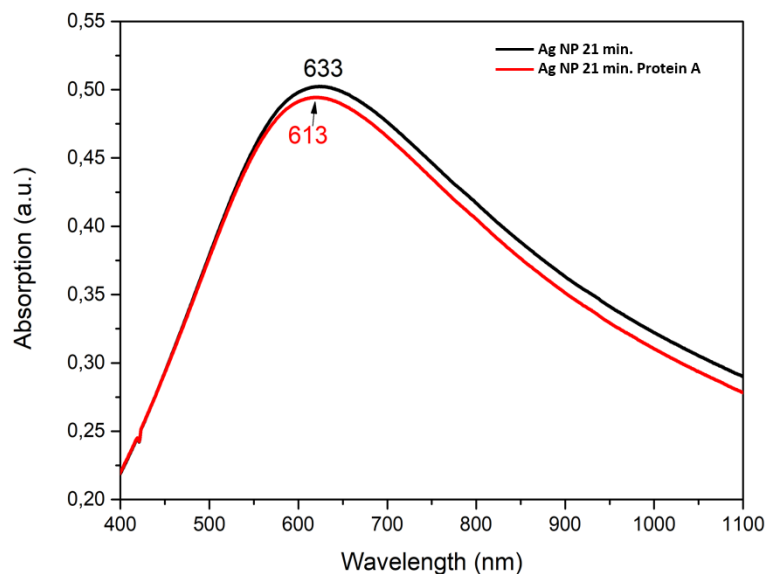


**Figure 9.** The UV-Vis spectrum of Ag and protein A binding NP produced by the PLD for 21 minutes (12600 laser pulses). The Ag NP with protein A is blue shifted for 20 nm.

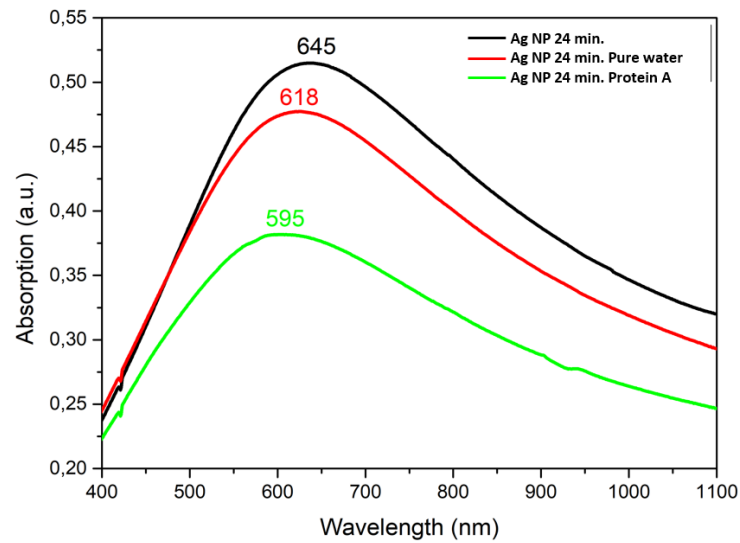


**Figure 10.** The UV-Vis spectrum of Ag, pure water and protein A binding NPs produced by the PLD for 24 minutes (14400 laser pulses). The pure water, and protein A binding NPs are blue shifted for 27 and 50 nm, respectively.

Figure 9 illustrates the UV-Vis spectrum of Ag and protein A binding NP produced by the PLD for 12600 laser pulses. The Ag NP with protein A is blue shifted for 20 nm. This suggests that the protein A molecules are bonded to the surface of the Ag NPs in the produced thin films. In addition of the LSPR peak shift of the Ag NPs with protein A, the full width at half maximum (FWHM) of the peak is measured to be changed. This may infer that the figure of merit for the produced Ag NP is suitable for a potential sensor.

The UV-Vis spectrum of pure Ag, Ag with pure water and Ag with protein A is shown in Figure 10. As Ag NPs are bounded by protein A, the LSPR peak blue-shift is around 50 nm. Ag NPs with pure water also shifts to blue side of the spectrum by 27 nm compared to the pure Ag NPs. In terms of refractive index unit (RIU), this corresponds to a wavelength shift around 100 nm/RIU.

#### 4. Conclusion

Ag NPs with different sizes and spherical shapes were produced by the PLD method. The produced Ag NPs were investigated by the UV-Vis spectrometer. The plasmonic LSPR peaks of Ag NPs were found to be positioned at 680 and 700 nm for deposition of 12600 and 14400 laser pulses, respectively. The morphology of Ag NPs was determined by the SEM images and it is found that the Ag NPs produced for 12400 laser pulses are relatively smaller than those of Ag NPs produced for 14400 laser pulses. When duration of deposition increases, the size of produced NPs increases. The EDX spectrum of both Ag NPs produced for 12600 and 14400 laser pulses are containing the expected elements of Ag and the ones that include in the composition of glass microscope slides. The wavelength shift of the LSPR peaks is examined by binding Ag NPs' surface by pure water and protein A. The resulting blue-shifts are 27 and 50 nm for 12600 and 14400 laser pulses, respectively. These results suggest that the produced Ag NPs could be employed as sensors for different biomolecules in the future experiments.

#### Acknowledgements

This work was supported by Dicle University Scientific Research Projects Coordinatorship under Project No FEN.20.006.

## Ethical Statements

The author declares that this document does not require an ethics committee approval or any special permission. Our study does not cause any harm to the environment.

## Conflict of interest

Authors declare no conflict of interest.

## Authors Contributions

IC, SYG and YG carried out the experiments and wrote the manuscript. HBG supervised the project. All authors discussed the results and contributed to the final manuscript.

## References

- [1] C.-T. Liu, and A.-N. Tang, "Applications of nanoparticles in elemental speciation," *Analytical Letters*, 48(7), 1031-1043, 2015.
- [2] N. Li, D. Liu, and H. Cui, "Metal-nanoparticle-involved chemiluminescence and its applications in bioassays," *Analytical and bioanalytical chemistry*, 406(23), 5561-5571, 2014.
- [3] C. L. Haynes, and R. P. Van Duyne, "Nanosphere lithography: a versatile nanofabrication tool for studies of size-dependent nanoparticle optics," ACS Publications, 2001.
- [4] A. R. Tao, S. Habas, and P. Yang, "Shape control of colloidal metal nanocrystals," *small*, 4(3), 310-325, 2008.
- [5] E. Ringe, B. Sharma, A.-I. Henry *et al.*, "Single nanoparticle plasmonics," *Physical Chemistry Chemical Physics*, 15(12), 4110-4129, 2013.
- [6] A. Powell, M. Wincott, A. Watt *et al.*, "Controlling the optical scattering of plasmonic nanoparticles using a thin dielectric layer," *Journal of Applied Physics*, 113(18), 184311, 2013.
- [7] A. L. González, C. Noguez, and A. S. Barnard, "Mapping the structural and optical properties of anisotropic gold nanoparticles," *Journal of Materials Chemistry C*, 1(18), 3150-3157, 2013.
- [8] T. Ahmad, I. A. Wani, J. Ahmed *et al.*, "Effect of gold ion concentration on size and properties of gold nanoparticles in TritonX-100 based inverse microemulsions," *Applied Nanoscience*, 4(4), 491-498, 2014.
- [9] W. A. Murray, B. Auguie, and W. L. Barnes, "Sensitivity of localized surface plasmon resonances to bulk and local changes in the optical environment," *The Journal of Physical Chemistry C*, 113(13), 5120-5125, 2009.
- [10] M. M. Miller, and A. A. Lazarides, "Sensitivity of metal nanoparticle surface plasmon resonance to the dielectric environment," *The Journal of Physical Chemistry B*, 109(46), 21556-21565, 2005.
- [11] A. C. Templeton, W. P. Wuelfing, and R. W. Murray, "Monolayer-protected cluster molecules," *Accounts of chemical research*, 33(1), 27-36, 2000.
- [12] M. A. El-Sayed, "Some interesting properties of metals confined in time and nanometer space of different shapes," *Accounts of chemical research*, 34(4), 257-264, 2001.
- [13] L. N. Lewis, "Chemical catalysis by colloids and clusters," *Chemical Reviews*, 93(8), 2693-2730, 1993.
- [14] T. Tani, *Silver nanoparticles: from silver halide photography to plasmonics*: Oxford University Press, USA, 2015.

- [15] S. R. Nicewarner-Pena, R. G. Freeman, B. D. Reiss *et al.*, "Submicrometer metallic barcodes," *Science*, 294(5540), 137-141, 2001.
- [16] S. A. Maier, M. L. Brongersma, P. G. Kik *et al.*, "Plasmonics—a route to nanoscale optical devices," *Advanced materials*, 13(19), 1501-1505, 2001.
- [17] P. V. Kamat, "Photophysical, photochemical and photocatalytic aspects of metal nanoparticles," ACS Publications, 2002.
- [18] C. Murray, S. Sun, H. Doyle *et al.*, "Monodisperse 3d transition-metal (Co, Ni, Fe) nanoparticles and their assembly into nanoparticle superlattices," *Mrs Bulletin*, 26(12), 985-991, 2001.
- [19] S. Nie, and S. R. Emory, "Probing single molecules and single nanoparticles by surface-enhanced Raman scattering," *science*, 275(5303), 1102-1106, 1997.
- [20] L. A. Dick, A. D. McFarland, C. L. Haynes *et al.*, "Metal film over nanosphere (MFON) electrodes for surface-enhanced Raman spectroscopy (SERS): Improvements in surface nanostructure stability and suppression of irreversible loss," *The Journal of Physical Chemistry B*, 106(4), 853-860, 2002.
- [21] K. M. Mayer, and J. H. Hafner, "Localized surface plasmon resonance sensors," *Chemical reviews*, 111(6), 3828-3857, 2011.
- [22] C. W. Hsu, B. G. DeLacy, S. G. Johnson *et al.*, "Theoretical criteria for scattering dark states in nanostructured particles," *Nano letters*, 14(5), 2783-2788, 2014.
- [23] T. R. Jensen, M. L. Duval, K. L. Kelly *et al.*, "Nanosphere lithography: effect of the external dielectric medium on the surface plasmon resonance spectrum of a periodic array of silver nanoparticles," *The Journal of Physical Chemistry B*, 103(45), 9846-9853, 1999.
- [24] K. Hamamoto, R. Micheletto, M. Oyama *et al.*, "An original planar multireflection system for sensing using the local surface plasmon resonance of gold nanospheres," *Journal of Optics A: Pure and Applied Optics*, 8(3), 268, 2006.
- [25] G. Mie, "Articles on the optical characteristics of turbid tubes, especially colloidal metal solutions," *Ann. Phys*, 25(3), 377-445, 1908.
- [26] I. Abdulhalim, M. Zourob, and A. Lakhtakia, "Surface plasmon resonance for biosensing: a mini-review," *Electromagnetics*, 28(3), 214-242, 2008.
- [27] D. R. Shankaran, K. V. Gobi, and N. Miura, "Recent advancements in surface plasmon resonance immunosensors for detection of small molecules of biomedical, food and environmental interest," *Sensors and Actuators B: Chemical*, 121(1), 158-177, 2007.
- [28] F. S. R. R. Teles, "Biosensors and rapid diagnostic tests on the frontier between analytical and clinical chemistry for biomolecular diagnosis of dengue disease: A review," *Analytica chimica acta*, 687(1), 28-42, 2011.
- [29] P. Leonard, S. Hearty, J. Brennan *et al.*, "Advances in biosensors for detection of pathogens in food and water," *Enzyme and Microbial Technology*, 32(1), 3-13, 2003.
- [30] A. Olaru, C. Bala, N. Jaffrezic-Renault *et al.*, "Surface plasmon resonance (SPR) biosensors in pharmaceutical analysis," *Critical reviews in analytical chemistry*, 45(2), 97-105, 2015.
- [31] R. G. Smith, N. D'Souza, and S. Nicklin, "A review of biosensors and biologically-inspired systems for explosives detection," *Analyst*, 133(5), 571-584, 2008.

- [32] W. Haiss, N. T. Thanh, J. Aveyard *et al.*, “Determination of size and concentration of gold nanoparticles from UV– Vis spectra,” *Analytical chemistry*, 79(11), 4215-4221, 2007.